

imposed d.c. field of 0.05 mT.

Figure 1 also gives results of measurements of  $\chi$ ,  $\chi_{fd}$  and  $\chi_{ARM}$  parameters plotted against the soil profile. The figure shows not only heating-induced enhancement of  $\chi$  as expected and observed by other workers but also significant enhancement of  $\chi_{fd}$  and  $\chi_{ARM}$ .

Banerjee *et al.*<sup>10</sup> have discussed the potential use of the  $\chi_{ARM}$  vs  $\chi$  plot for magnetic granulometry. King *et al.*<sup>11</sup> have constructed a simple phenomenological model (figure 1b of ref. 11) based on measurement of these parameters on magnetite powders of different grain sizes. This model shows that in magnetite, fining the magnetic grain size increases the slope of the straight-line plot of  $\chi_{ARM}$  vs  $\chi$ .

Following the model of King *et al.*<sup>11</sup> we have plotted  $\chi_{ARM}$  vs  $\chi$  for both unheated and heated soil samples (Figure 2). It can be seen that there is a marked increase of slope of the straight line for the heated samples. This is further evidence for the generation of secondary ultrafine ferrimagnetic grains in soils consequent upon heating.

In conclusion, we have shown evidence for the enhancement in the proportion of ultrafine ferrimagnetic grains during the process of heating of soils. The enhancement is independent of the chemical environment and thus appears to be due to breaking down of the domains during the process of heating.

1. Mullins, C. E. and Tite, M. S., *J. Geophys. Res.*, 1973, **78**, 804.
2. Thompson, R. and Oldfield, F., *Environmental Magnetism*, Allen and Unwin, London, 1986, p. 227.
3. Kirschvink, J. L. and Chang, S. B. R., *Geology*, 1984, **12**, 559.
4. Maher, B. A. and Taylor, R. M., *Nature*, 1988, **336**, 368.
5. Le Borgne, E., *Ann. Geophys.*, 1955, **11**, 399.
6. Mullins, C. E., *J. Soil Sci.*, 1977, **28**, 223.
7. Ozdemir, O. and Banerjee, S. K., *Earth Planet. Sci. Lett.*, 1982, **59**, 393.
8. Oldfield, F., Thompson, R. and Dickinson, D. P. E., *Phys. Earth Planet. Int.*, 1981, **26**, 107.
9. Tite, M. S. and Lington, E. E., *Nature*, 1975, **256**, 565.
10. Banerjee, S. K., King, J. and Marvin, J., *Geophys. Res. Lett.*, 1981, **8**, 333.
11. King, J., Banerjee, S. K., Marvin, J. and Ozdemir, O., *Earth Planet. Sci. Lett.*, 1982, **59**, 404.

ACKNOWLEDGEMENT. The soil samples used in this study were collected under the aegis of the Kashmir Palaeoclimate Project funded by the Department of Science and Technology, New Delhi.

16 January 1990

## Estimation of cyclone heat potential over Bay of Bengal using satellite and ship data

K. A. Dhoulath, M. M. Ali,\* P. S. Desai\* and P. G. Kurup

Physical Oceanography and Meteorology Division, Cochin University of Science and Technology, Cochin 682 016, India

\*Meteorology and Oceanography Division, Space Applications Centre, Ahmedabad 380 053, India

Monitoring of large-scale climate-related variability over the ocean from space using remote-sensing techniques allows the global coverage needed for climate studies. Using satellite-derived sea surface temperature (SST) and wind speed, cyclone heat potential (CHP<sub>28</sub>) was estimated utilizing a regression analysis obtained from ship-derived CHP<sub>28</sub>, wind speed and SST. CHP<sub>28</sub> from satellite data has been compared with ship-derived CHP<sub>28</sub> and found to be within  $\pm 10\%$  of the latter. Analysis of variation of CHP<sub>28</sub> over western Bay of Bengal before and after a cyclonic storm shows that the storm heat potential increased towards the storm area, while after the storm it decreased.

STUDIES on the heat content of the surface mixed layer of the oceans have received considerable attention in recent years because of its importance in ocean-atmosphere energy exchanges. It is known that long-period weather fluctuations are related to the larger thermal memory of the oceans. Heat storage in the upper layer has a pronounced effect on the Indian monsoonal forcing. The annual heat content variations of this layer appear to be mainly due to vertical movement of the thermocline associated with the dynamics of seasonal winds<sup>1</sup>. Large-scale sea surface temperature (SST) changes have been found to affect cyclone tracks and related monsoon activity<sup>2</sup>.

Cyclone heat potential of the ocean may be defined as the heat content from the surface to a particular isothermal depth, e.g. the 28°C isotherm<sup>3</sup> (CHP<sub>28</sub>) or the 26°C isotherm<sup>4</sup>. Surface wind and SST are the key factors controlling CHP<sub>28</sub>.

Cyclone heat potential over the Indian Ocean has earlier been estimated by conventional methods using vertical temperature profiles<sup>3,4</sup>. Some attempts have recently been made to estimate the heat content of the oceans using satellite data. Christensen and Mascarenhas<sup>5</sup> calculated the heat storage by attributing the density anomaly to temperature only. Miller<sup>6</sup> developed a one-dimensional model of the upper-ocean mixed layer and an algorithm that uses satellite-derived wind stress and SST to predict real-time changes in upper-ocean heat storage during cooling seasons. The present attempt is to estimate cyclone heat potential in the western Bay of Bengal

during a premonsoon cyclonic disturbance of May 1979, using NOAA-derived SST and surface wind speed obtained by extrapolating GOES low-level cloud motion vector winds to the surface<sup>7</sup>. This method holds good for the period May–July and for 700–900 mb level winds with an r.m.s. difference of 2.6 m s<sup>-1</sup>. NOAA-derived SST-values have been corrected for water vapour following Pathak<sup>8</sup>.

Hydrographic data of MONEX-79 (May–July) were used to estimate CHP<sub>28</sub> by the conventional methods. Satellite data of GOES low-level cloud motion vector winds extrapolated to the surface and NOAA-derived SST and water vapour over the Bay of Bengal were utilized for the regression analysis. Station location and the track of the premonsoon cyclonic disturbance are shown in Figure 1.

*Estimation of CHP<sub>28</sub> using ship data.* The cyclone heat potential of the 28°C isotherm was estimated as

$$CHP_{28} = \rho C_p \int_0^{D_{28}} t_z dz,$$

where  $\rho$  is the density of water,  $C_p$  the specific heat at constant pressure,  $D_{28}$  the depth of the 28°C isotherm, and  $t_z$  the average temperature of the layer  $dz$ . The 28°C isotherm was chosen as most of the tropical cyclones are formed when SST  $\geq$  28°C (ref. 3). The factor  $\rho C_p$  was taken as 0.977 cal/cm<sup>3</sup>/°C following Bathen<sup>9</sup>.

*Extrapolation of GOES cloud motion vector winds.* GOES 900 mb cloud motion vector winds were extrapolated to the surface using the relation<sup>7</sup>

$$W_s = 0.72 W_c + 1.2,$$

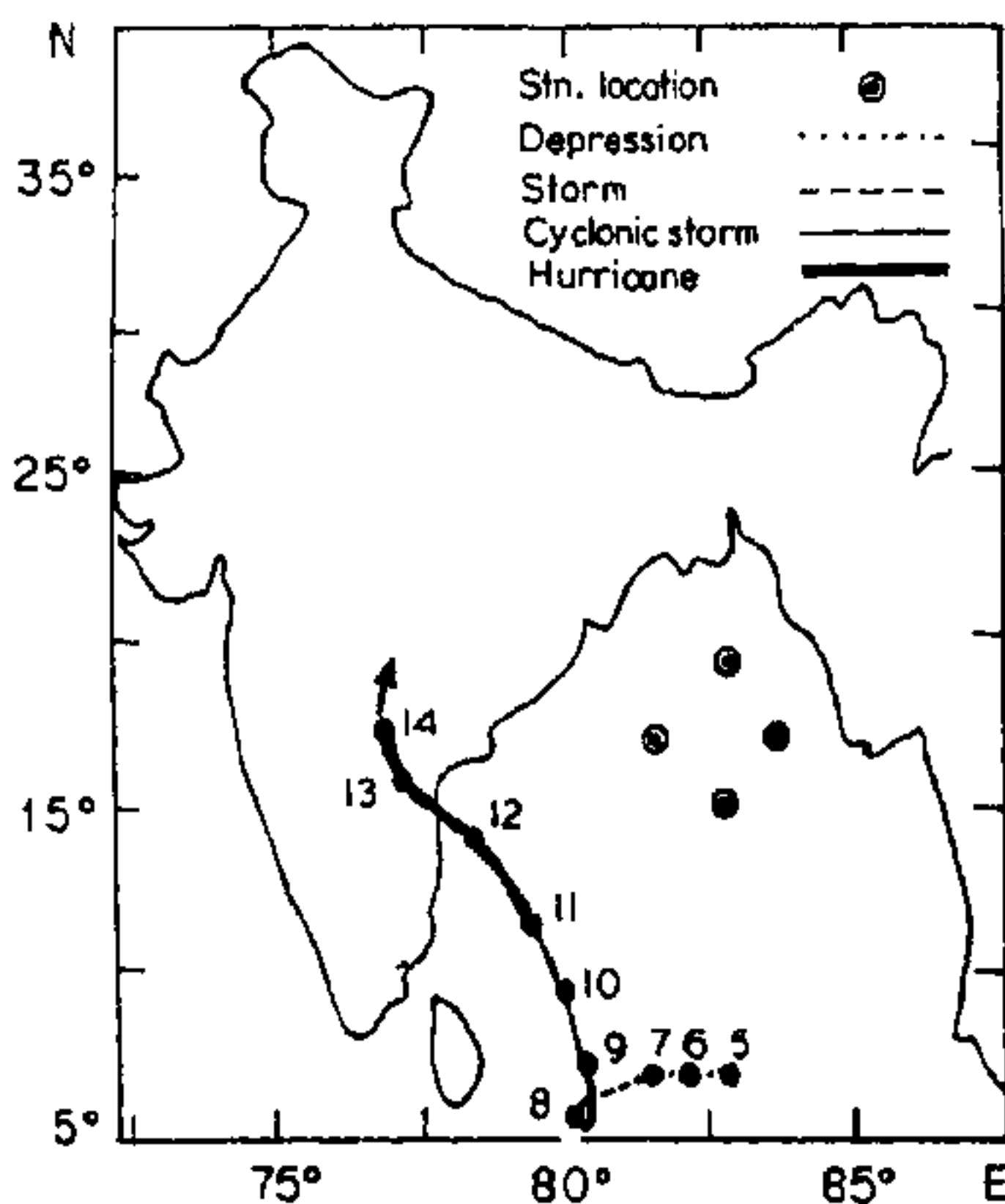


Figure 1. Map showing the track of pre-monsoon cyclonic disturbance (May 1979) and location of hydrographic stations.

where  $W_s$  is the surface wind speed and  $W_c$  the wind speed derived from cloud motion at the cloud level in m s<sup>-1</sup>.

*Correction of NOAA-derived SST.* SST values obtained as finished data products from NOAA differ, on an average, by 1.5°C from the in situ observations<sup>8</sup>. The differences in SST and the total water vapour content of the atmosphere are empirically related by

$$T_s = T_{SAT} + 0.13 W_v - 5.1,$$

where  $T_s$  is the corrected SST,  $T_{SAT}$  the SST before correction, and  $W_v$  the water vapour content in millimetres of precipitable water<sup>8</sup>.

*Estimation of CHP<sub>28</sub> from satellite data.* To estimate CHP<sub>28</sub> from satellite-derived values of SST and wind speed, a regression analysis was carried out between values of CHP<sub>28</sub> estimated from hydrographic data and the measured values of SST and wind speed. The regression equation is of the form.

$$CHP_{28} = A + BW + CT,$$

where  $A = -0.5030$ ,  $B = 120.22$ ,  $C = 6988.88$ ,  $W$  is the surface wind speed, and  $T$  the SST. Using the satellite-derived values of wind speed ( $W_s$ ) and SST ( $T_s$ ) corrected for water vapour instead of  $W$  and  $T$ , CHP<sub>28</sub> was estimated from the regression equation. The satellite-derived CHP<sub>28</sub> values were averaged daily in 1° × 1° grids and the values interpolated corresponding to the ship-derived CHP<sub>28</sub> values.

The regression formula developed in the present study is based on 466 data points (using hydrographic data) with an r.m.s. difference of 1512 cal cm<sup>-2</sup> and a correlation coefficient equal to 0.9682. Owing to lack of simultaneous observations of satellite and ship, CHP<sub>28</sub> estimated using satellite-derived SST and wind speed were compared at nine points with the values estimated from hydrographic data (Table 1). The scatter plot for the two is shown in Figure 2. The values obtained using

Table 1. Comparison of CHP<sub>28</sub> estimated from satellite-derived parameters and from ship measurements (kcal cm<sup>-2</sup>)

Estimated CHP <sub>28</sub>		
Satellite-derived	Ship-derived	Difference
18.0	15.9	2.1
14.5	13.9	0.6
13.8	14.0	0.2
14.0	15.0	1.0
11.4	16.0	4.6
13.8	15.3	1.5
14.7	15.3	0.6
16.7	16.0	0.7
18.7	16.1	2.6
Mean 15.1	15.3	1.5



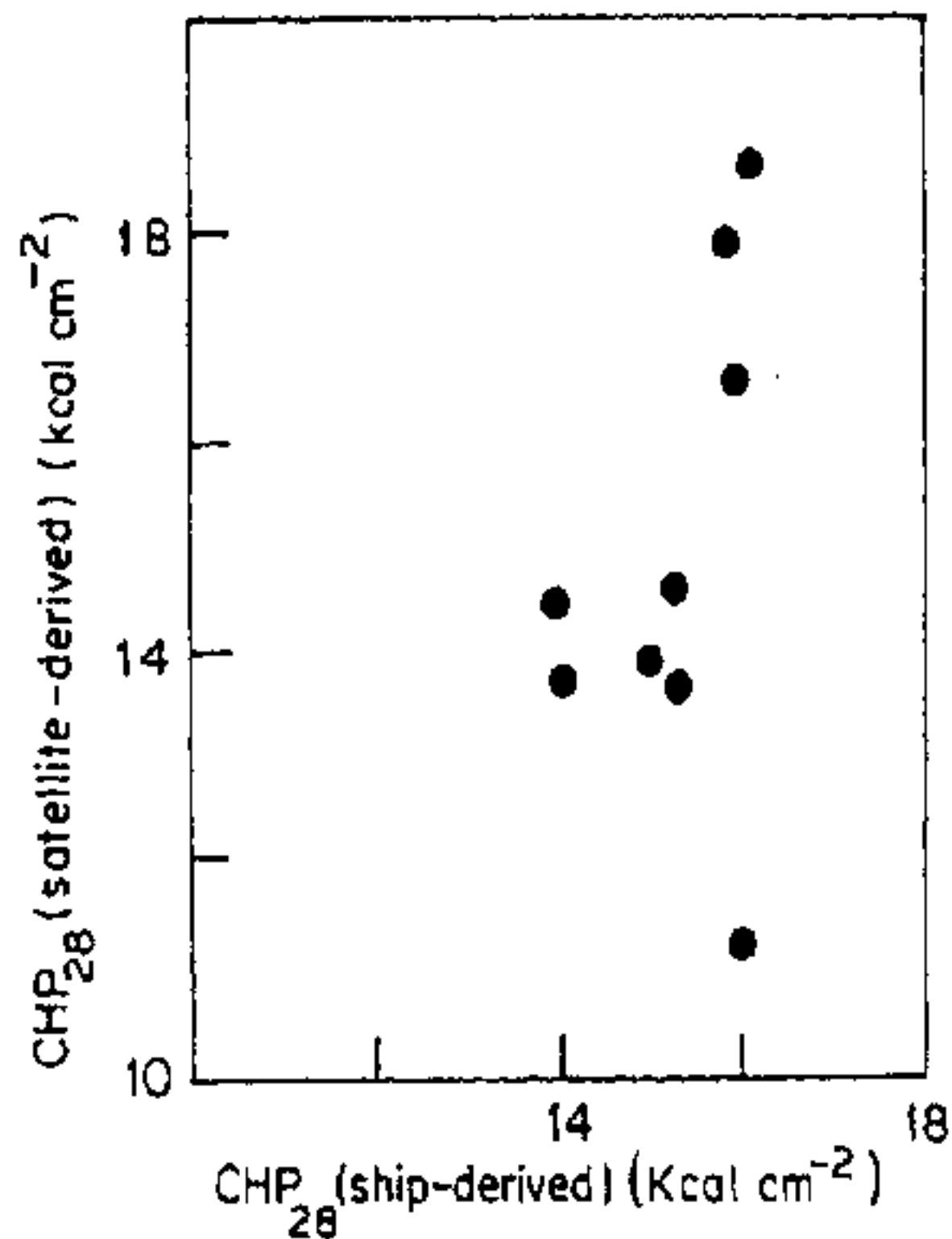


Figure 2. Scatter between ship- and satellite-derived CHP<sub>28</sub> values (kcal cm<sup>-2</sup>)

satellite-derived parameters and those from ship data are comparable (within  $\pm 10\%$ ). At three points the variations of CHP<sub>28</sub> are wider; this can be expected considering that wind speeds have been obtained by extrapolating cloud motion vector winds to the surface.

The role of ocean heat potential in atmospheric disturbances was examined using information from Indian Daily Weather Reports on the severe cyclonic storm that formed in the southwestern Ba of Bengal during 5-13 May 1979.

The well-marked low pressure, which intensified into a depression on the evening of 5 May, lay around 7°N,90°E. Moving slowly westwards, the depression developed into a storm by the morning of 7 May near

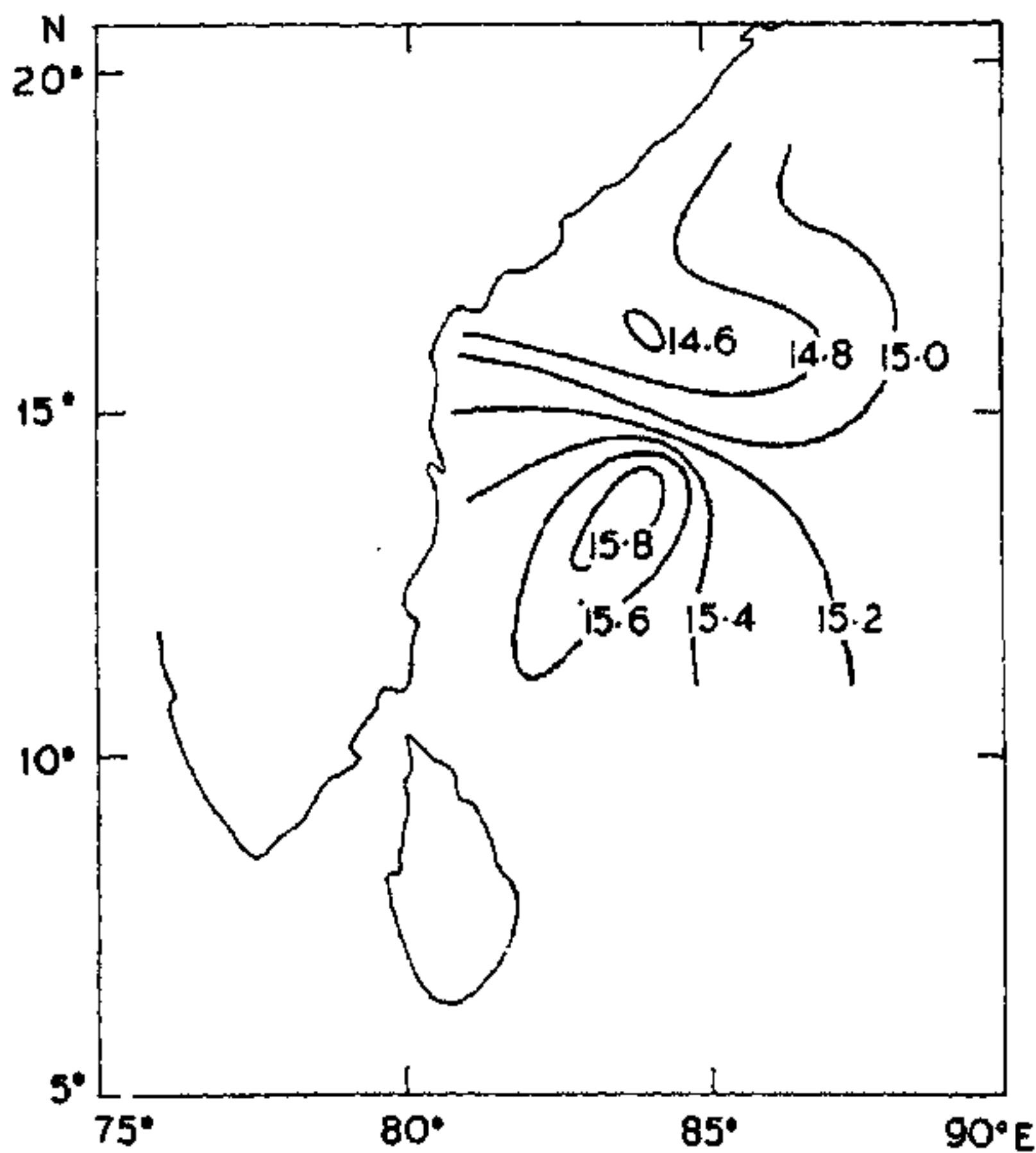


Figure 3a. Distribution of cyclone heat potential (kcal cm<sup>-2</sup>) over southwestern Bay of Bengal on 1 May 1979.

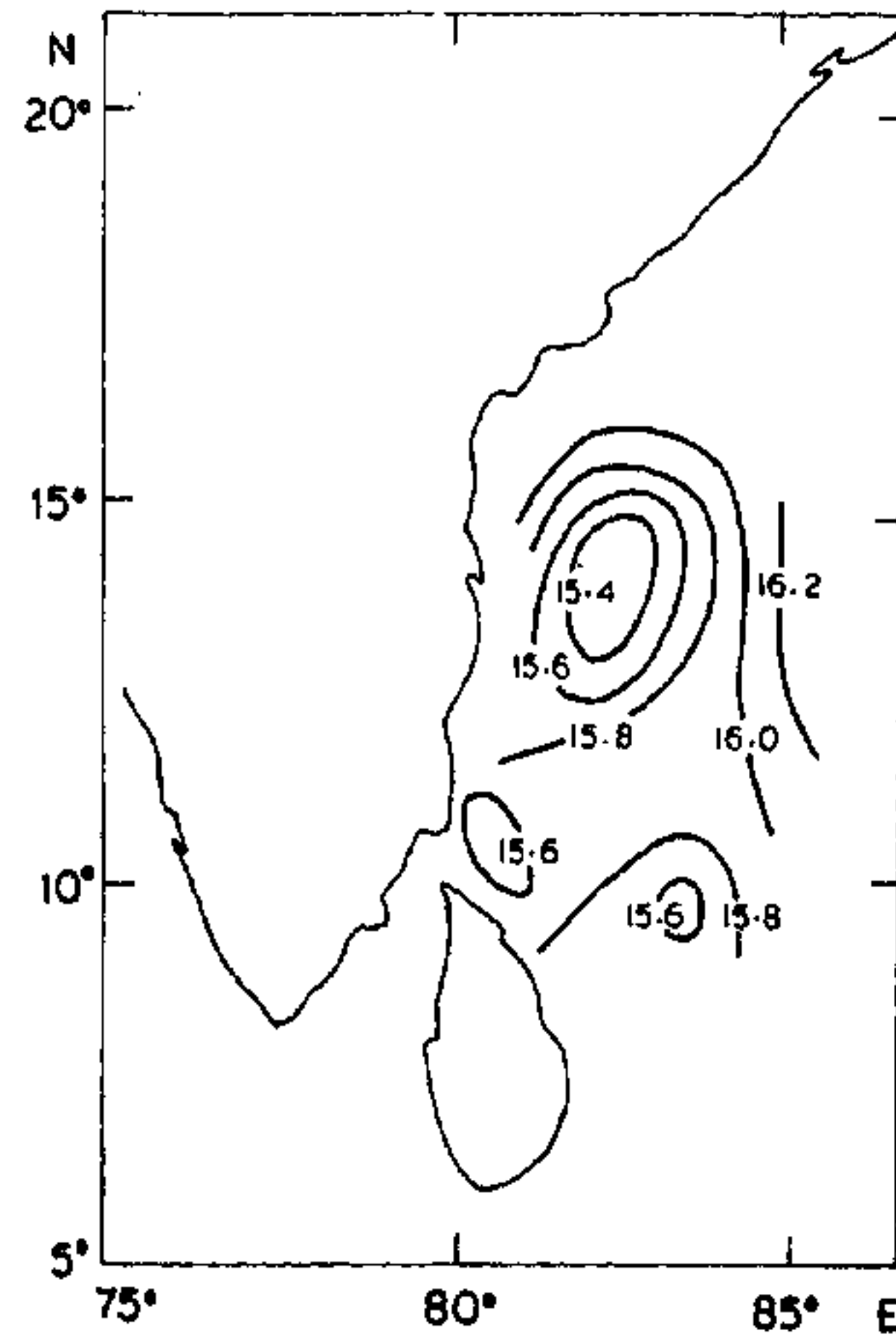


Figure 3b. Distribution of cyclone heat potential (kcal cm<sup>-2</sup>) over southwestern Bay of Bengal on 17 May 1979.

7°N,88°E. The storm took a westsouthwesterly track and developed into a cyclonic storm by the morning of 8 May. It then moved northwestwards upto the morning of 11 May and developed into a hurricane with maximum intensity on 11 and 12 May. It crossed the Andhra coast between Nellore and Ongole by the evening of 12 May and gradually dissipated by the morning of 14 May (Figure 1).

Figure 3 shows the distribution of CHP<sub>28</sub> on 1 May and 17 May 1979 (4 days before and after the storm). On 1 May, the heat potential increased in the southwesterly direction, reaching a maximum value of 15.8 kcal cm<sup>-2</sup> around 13.5°N,83°E. This increase in CHP<sub>28</sub>

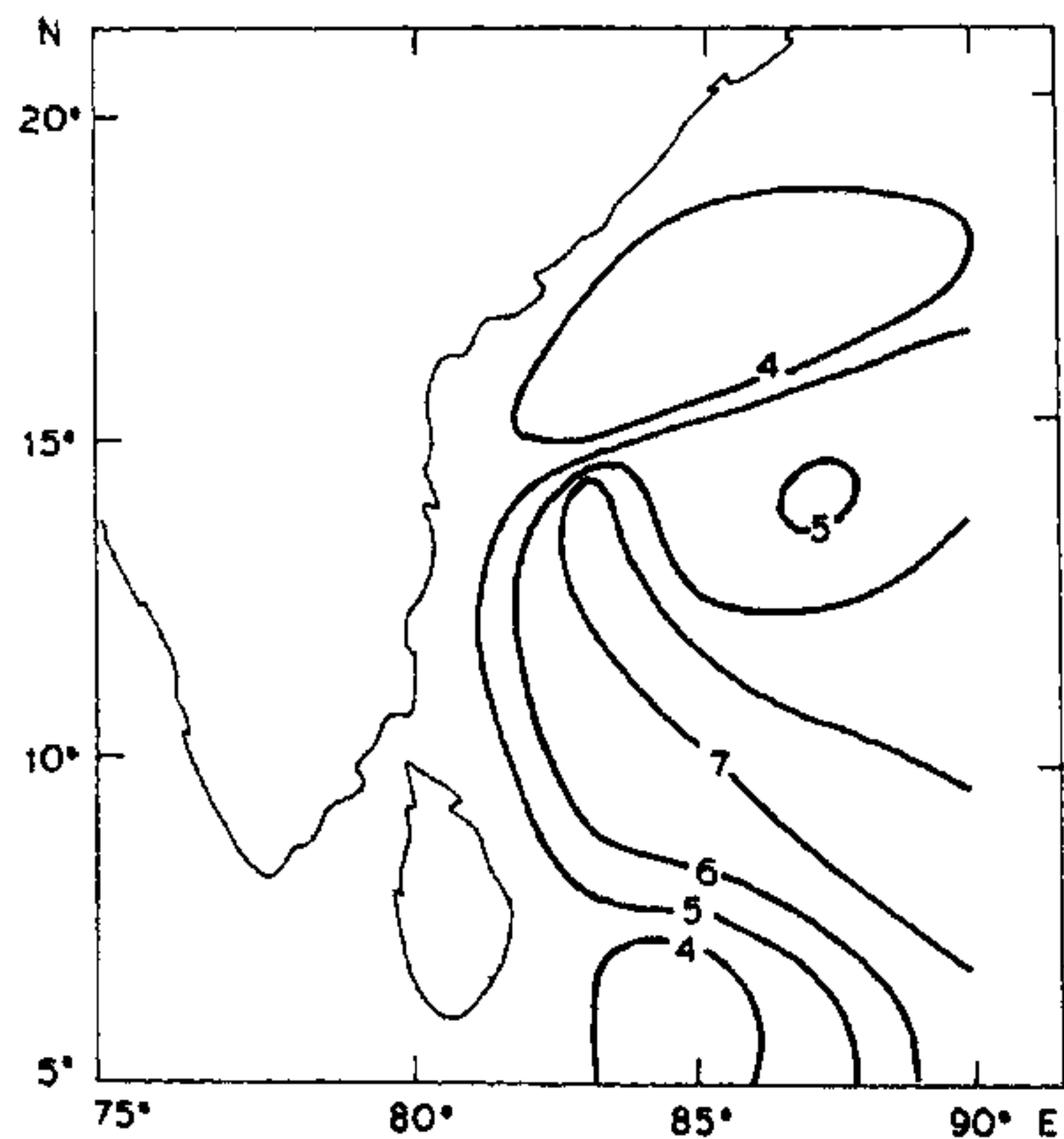


Figure 4a. Distribution of surface wind speed (ms<sup>-1</sup>) over southwestern Bay of Bengal on 1 May 1979.

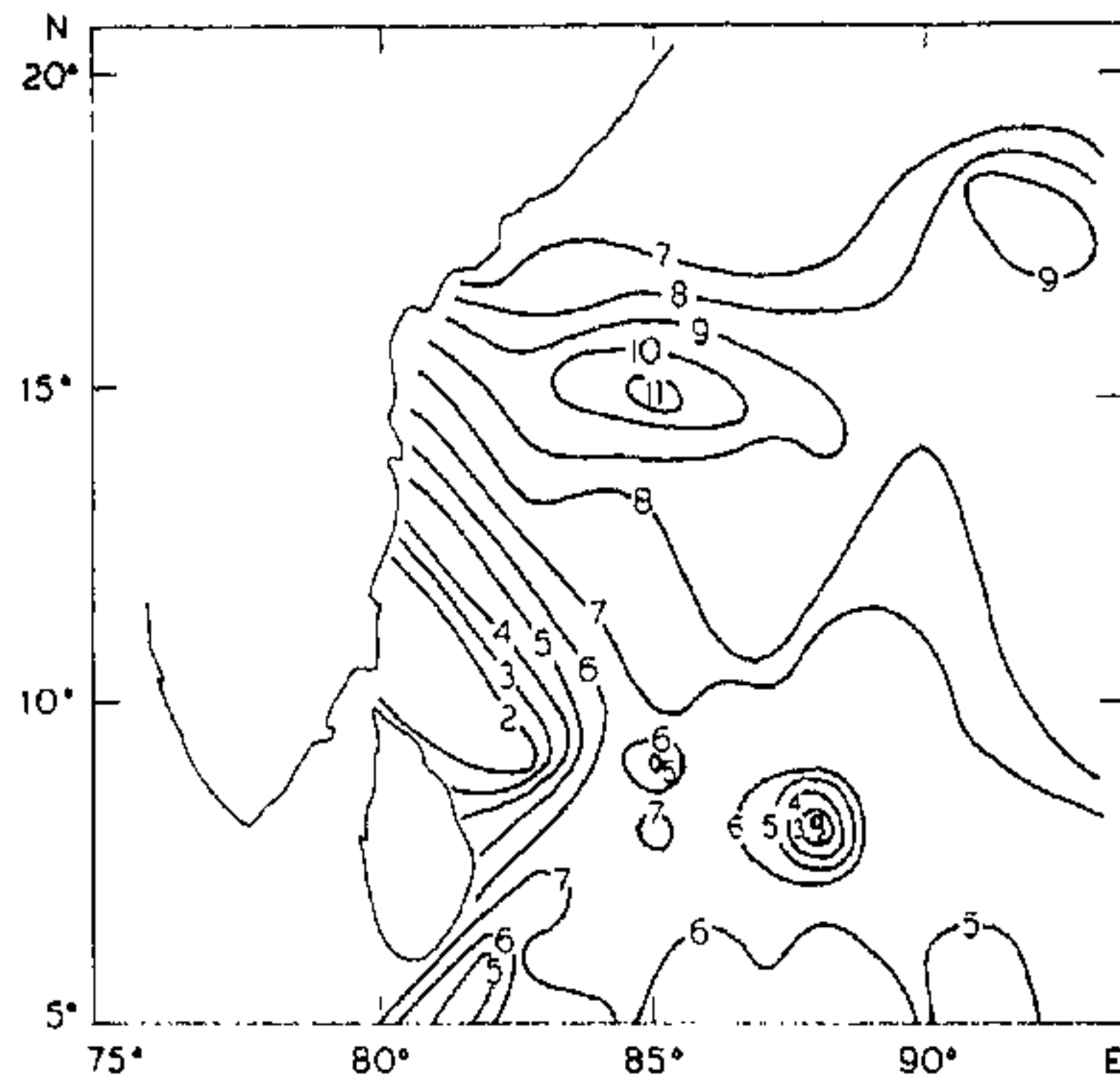


Figure 4b. Distribution of surface wind speed ( $\text{ms}^{-1}$ ) over southwest Bay of Bengal on 17 May 1979.

may be a result of deep MLD and high SST, providing a favourable condition for the formation of a depression. The low heat potential observed on 17 May could be because of heat taken by the storm in the form of latent heat as this area of low heat potential is along the track of the cyclone. Gradual decrease in cyclone heat potential due to the movement of a disturbance across the east central Arabian Sea has been reported earlier<sup>4</sup>.

Figure 4 shows the distribution of surface wind speed on 1 and 17 May over the study area. Near the central Bay, wind speed is very low. In the southeastern direction contours are widely spaced, indicating less variation. Wind speed increases rapidly towards west, reaching a maximum value of  $7.6 \text{ ms}^{-1}$  at  $14^{\circ}\text{N}, 83^{\circ}\text{E}$ . Comparing this with Figure 3a, it is seen that, for both wind speed and  $\text{CHP}_{28}$ , the trends of the gradient are same. On 17 May, wind speed increases in the direction of passage of the storm. Maximum wind speed occurs near  $15^{\circ}\text{N}, 85^{\circ}\text{E}$ , coinciding with the area of maximum  $\text{CHP}_{28}$ .

1. Merle, J., *J. Phys. Oceanogr.*, 1981, **10**, 464.
2. Joseph, P. V., *Mausam*, 1980, **32**, 237.
3. Rao, R. R., *Mausam*, 1984, **38**, 147.
4. Ramesh Babu and Sastry, J. S., *Mausam*, 1984, **35**, 17.
5. Christensen, E. N. and Mascarenhas, A. S., *Science*, 1979, **203**, 653.
6. Miller, J. R., *Remote Sensing of Environ.*, 1984, **11**, 173.
7. Wylie, D. P. and Hinten, B. B., *Boundary Layer Met.*, 1982, **23**, 197.
8. Pathak, P. N., *Remote Sensing of Environ.*, 1982, **12**, 363.
9. Bathen, K. H., *J. Geophys. Res.*, 1971, **76**, 676.

ACKNOWLEDGEMENTS. We thank Dr P. P. Kale, Director, Space Application Centre, Ahmedabad, for providing computer facilities and MONEX-79 data, and the Department of Ocean Development, New

Delhi, for financial support.

11 March 1989; revised 5 September 1989.

## Long-term wave statistics off Goa

G. Muraleedharan, N. Unnikrishnan Nair\* and P. G. Kurup

Physical Oceanography and Meteorology Division, School of Marine Sciences, Cochin University of Science and Technology, Cochin 682 016, India

\*Department of Mathematics and Statistics, Cochin University of Science and Technology, Cochin 682 022, India

Long-term wave statistics from grid 9 (NPOL Atlas) and grid XIII (NIO Atlas) off Goa were examined and compared with recorded wave information. Wave directions and average monthly frequency of waves in the period 5 to 8 sec (zero-crossing period) from grid XIII were comparable with recorded information at Goa. The theoretical and calculated values of significant wave heights were in agreement for grid 9. The wave power averaged from swell statistics (grid XIII) was found to be much higher than that averaged from sea and swell statistics (grid 9).

A knowledge of wave climate is important from the strategic, economic and commercial points of view. Different workers<sup>1,2</sup> have pointed out that visual observations suggest a reasonable representation for wave climatological studies. Here an attempt was made to study the wave climatology for an area off Goa by utilizing the available wave atlases and recorded information.

Visual wave parameters obtained from grid 9 ( $13^{\circ}$ – $17^{\circ}\text{N}$ ,  $73^{\circ}$ – $74.7^{\circ}\text{E}$ ) (NPOL Atlas, 1978) and grid XIII ( $15^{\circ}$ – $20^{\circ}\text{N}$ ,  $70^{\circ}$ – $74^{\circ}\text{E}$ ) (NIO Atlas, 1982) were utilized in the present work<sup>3,4</sup> (Figure 1). These grids overlap over an area off Goa. Wave direction, wave power and percentage frequency of occurrence of waves in the period range 5 to 8 sec (zero-crossing period) from these grids were examined in the light of recorded information off Goa<sup>5</sup>. Zero-crossing period is the average of zero up-crossing period (the time difference between two consecutive points at which the wave crosses the mean sea level in the upward direction) and zero down-crossing period (the time difference between two consecutive points at which the wave crosses the mean sea level in the downward direction). Wave power was calculated using the relation

$$P = 0.55 H_s^2 T_z, \quad (1)$$

where  $P$  is the power available on a random sea<sup>6</sup>,  $H_s$  the significant wave height and  $T_z$  the zero-crossing period, computed from the relation<sup>7</sup>

$$T_s = 1.3T_z - 2.5, \quad (2)$$

where  $T_s$  is the significant wave period, The wave heights